Optimized Time Splitting to Maximize the Lower Bound of Rate with Channel Estimation in an Interference Alignment Based Network

Rugui YAO [1], *Lukun YAO* [1], *Juan XU* [2], *Xiaoya ZUO* [1], *Hailong LIU* [1]

[1] School of Electronics and Information, Northwestern Polytechnical University, 710072 Xi'an, Shaanxi, China
[2] School of Electronic and Control Engineering, Chang'an University, 710064 Xi'an, Shaanxi, China

yaorg@nwpu.edu.cn, ylk@mail.nwpu.edu.cn, xuj@mail.nwpu.edu.cn, zuoxy@nwpu.edu.cn

Submitted July 25, 2018 / Accepted December 6, 2018

Abstract. *In this paper, for an interference alignment (IA) based network, a time splitting scheme for transmitting training and data symbols is optimized. The time allocated for transmitting training symbol will affect the precision of channel estimation (CE) and thus the achievable rate as well as the duration for data symbol transmission. With the least square (LS) and relaxed minimum mean square error (RMMSE) CE algorithm, the lower bounds of achievable rate are carefully derived, respectively. Then we formulate an optimization problem to maximize the lower bounds of achievable rate by optimizing the time splitting factor (TSF). The existence of optimum is first proved. Then, regarding the complexity of solution, Taylor expansion is adopted to find the approximated optimal TSF. Numerical results are presented to show the optimal TSF can achieve larger lower bound of achievable rate over other fixed TSFs due to its adaptivity to the channel characteristics and its statistics of CE errors. Numerical results also validate that the approximation just brings out some small and acceptable errors on the system rate. In addition, RMMSE CE algorithm shows better performance than LS CE because RMMSE considers noise statistics as modification.*

Keywords

Time splitting, lower bound, interference alignment, Taylor expansion

1. Introduction

Interference alignment (IA) is a promising technology for interference management in the wireless communications [1]. Different from interference avoidance of orthogonalizing the channel access, IA can limit all the interference to one half of the signal subspace and the other half can be used to transmit the desired signal without interference [2], [3]. The study of IA has attracted a lot of attentions for its good performance in improving the system rate.

In a multiple-input multiple-output (MIMO) interference network, two easily implemented algorithms were proposed to obtain the solutions of IA iteratively under the assumption of perfect channel state information (CSI) in [4], which can maximize the total achievable rate. However, due to the estimation error, quantization error, or feedback delay in practical applications, the instant CSI used is always imperfect. With the imperfect CSI, the IA performance is deteriorating sharply and even not better than traditional orthogonal methods [5]. Then, the robust design and performance evaluation of IA with imperfect CSI have been widely studied in [6–10]. For example, a novel IA scheme with imperfect CSI based on antenna selection was proposed to improve the received signal to interference plus noise ratio (SINR) in [6]. In [8], the average achievable rate of IA was provided considering channel estimation errors. Further in [9], the lower bound of capacity for IA with CSI errors are derived.

The above studies on IA with imperfect CSI are mostly based on the fixed duration training. In the information processing or communication system design, the system performance can be improved by optimizing some parameters [11–13]. In this paper, we introduce the time splitting factor (TSF) as the optimization variable. We can adjust the duration allocated to the training and data symbols' transmission to maximize the achievable rate for the network. For a given coherent time, if the allocated training duration is too short, more errors will be generated for the estimated CSI, which degrades the achievable system rate. On the contrary, if the training duration is too long, the duration for data symbol transmission will be shortened, also resulting in the decrease of data rate [3, 14, 15]. Therefore, how to perform the optimal time splitting for the training and data symbols transmission is quite important to achieve high rate.

In this paper, we evaluate the statistics property of the imperfect CSI due to practical channel estimation (CE) algorithm, such as least square (LS) and relaxed minimum mean square error (RMMSE) CE algorithm. With the different statistics of CE error for LS and RMMSE CE algorithm, the upper bound of interference leakage are derived respec-

tively [16]. Then, we propose an optimization problem of time splitting for the training and data symbols transmission to maximize the lower bound of achievable rate. For low complexity, Taylor expansion is applied to obtain the approximated optimal TSF. Finally, some numerical results are presented to validate the correctness of our proposed scheme.

The organization of the paper is as follows. In Sec. 2, the system model is presented and the received signal model is derived. Then we formulate the optimization problem and apply Taylor expansion to obtain the approximated optimal TSF in Sec. 3. In Sec. 4, numerical results are presented to validate the correctness and effectiveness of our scheme. Finally, Section 5 concludes the paper and schedules some future work.

2. System Model

In this paper, we consider an interference alignment based network, as shown in Fig. 1. The system includes K ($K > 1$) user pairs, sharing the same frequency band. Each user pair contains a transmitter, $\mathbf{T}_i$, equipped with m antennas and its intended receiver, $\mathbf{R}_i$, equipped with n antennas, for $i = 1, \cdots, K$. Each transmitter transmits only one data stream, that is, $d = 1$. In this study, we consider a slow block fading channel model where a CE is valid throughout the duration of the coherence time, which is assumed to be T symbol periods. Let $\alpha \in (0, 1)$ be the TSF, such that the training time is αT symbol periods, and the signal transmission time is $(1 - \alpha)T$ symbol periods.

The received signal at the k-th receiver, $\mathbf{y}_k \in C^{n\times 1}$, can be expressed as

$$\mathbf{y}_k = \sum_{l=1}^{K} \mathbf{H}_{kl}\mathbf{x}_l + \mathbf{n}_k \tag{1}$$

where $\mathbf{H}_{kl} \in C^{n\times m}$, $l, k = 1, \cdots, K$ is the channel matrix from the l-th transmitter to the k-th receiver, $\mathbf{n}_k \in C^{n\times 1} \sim \mathcal{CN}(\mathbf{0}, N_0\mathbf{I})$ represents the additive white Gaussian noise (AWGN) at the k-th receiver with N_0 being the noise power, and $\mathbf{x}_l \in C^{m\times 1}$ denotes the transmitted signal vector. Let $\mathbf{s}_l \in C^{d\times 1}$ be the transmitted symbol vector of the l-th transmitter. Let $\mathbf{V}_l \in C^{m\times d}$ be the precoding matrix for the l-th transmitter based on IA technique. Then we have

$$\mathbf{x}_l = \mathbf{V}_l\mathbf{s}_l, \tag{2}$$

where $\mathbf{s}_l \in C^{d\times 1}$ is the transmitted symbol vector of the l-th transmitter. Assuming that all transmitters have the same average power constraint, $\mathbb{E}\left\{\|\mathbf{s}_l\|_2^2\right\} \le \varepsilon$, $l = 1, \cdots, K$.

Considering the practical applications, the CSIs are obtained by the CE, quantization and feedback. Thus, some errors, i.e., imperfect CSIs, are emerged for the system design. In this paper, we model the imperfect CSI as

$$\mathbf{H}_{kl} = \hat{\mathbf{H}}_{kl} + \Delta\mathbf{H}_{kl} \tag{3}$$

where $\hat{\mathbf{H}}_{kl}$ is the estimated channel matrix and $\Delta\mathbf{H}_{kl}$ denotes the channel errors.

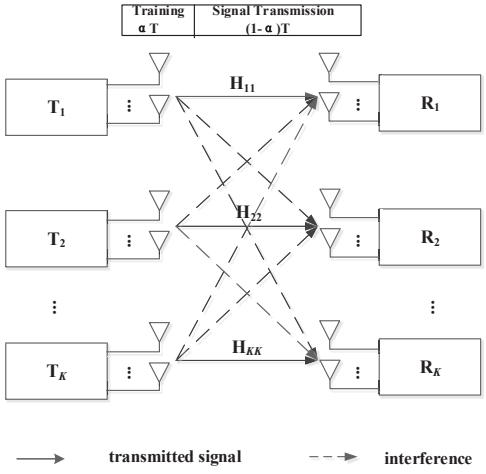

Fig. 1. System model.

Substituting (2), (3) into (1) and considering the receiving filter matrix $\mathbf{U}_k \in C^{n\times d}$ for IA, the received signal model in (1) is formulated as

$$\begin{aligned}\mathbf{U}_k^{\mathrm{H}}\mathbf{y}_k &= \sum_{l=1}^{K} \mathbf{U}_k^{\mathrm{H}}\hat{\mathbf{H}}_{kl}\mathbf{V}_l\mathbf{s}_l + \sum_{l=1}^{K} \mathbf{U}_k^{\mathrm{H}}\Delta\mathbf{H}_{kl}\mathbf{V}_l\mathbf{s}_l + \mathbf{U}_k^{\mathrm{H}}\mathbf{n}_k \\ &= \mathbf{U}_k^{\mathrm{H}}\hat{\mathbf{H}}_{kk}\mathbf{V}_k\mathbf{s}_l + \sum_{l=1}^{K} \mathbf{U}_k^{\mathrm{H}}\Delta\mathbf{H}_{kl}\mathbf{V}_l\mathbf{s}_l + \mathbf{U}_k^{\mathrm{H}}\mathbf{n}_k. \end{aligned} \tag{4}$$

In the second equation in (4), all the signal from other user pairs, $\sum_{l=1,l\neq k}^{K} \mathbf{U}_k^{\mathrm{H}}\hat{\mathbf{H}}_{kl}\mathbf{V}_l\mathbf{s}_l$, can be removed due to the IA design based on $\hat{\mathbf{H}}_{kl}$.

To better analyze the impact of channel errors, as in [17], we introduce error bound for $\Delta\mathbf{H}_{kl}$, δ_{kl}^2, which can be defined as

$$\delta_{kl}^2 = \max_i \|(\Delta\mathbf{H}_{kl})_i\|_2^2 \tag{5}$$

where $(\Delta\mathbf{H}_{kl})_i$ denotes the i-th row of $\Delta\mathbf{H}_{kl}$.

3. Optimization for Time Splitting Factor

3.1 Optimization Problem Formulation

As stated in Sec. 2, CE error has a large impact on the achievable system performance. Besides, the duration allocated to CE affects the precision of CE, i.e., CE error. The longer duration the CE procedure takes, the more precise CE we obtain, which helps to improve the achievable system rate. On the contrary, the longer CE duration causes shorter duration for data symbol transmission, which decreases the system rate instead. Therefore, we should optimize the TSF to trade-off the CE precision and the achievable system rate.

Note that, due to the randomness of CE error, we cannot easily evaluate the instantaneous achievable system rate. Generally, the ergodic rate [18] or lower bound of achievable

rate are adopted. In this paper, the lower bound of achievable rate, $R_k^{\mathrm{L}}(\alpha)$, is selected as the objective to optimize the TSF. Therefore, we formulate the optimization problem as

$$\begin{aligned} &\alpha_{\mathrm{opt}} = \arg\max_{\alpha} R_k^{\mathrm{L}}(\alpha) \\ &\text{s.t.} \quad \alpha \in (0,1). \end{aligned} \tag{6}$$

Considering the characteristics of CE error in (5), the TSF and the received signal model in (4), the lower bound of the achievable rate for the k-th user pair is calculated as [9]

$$R_k^{\mathrm{L}}(\alpha) = (1-\alpha)\log_2\left(1 + \frac{\left(\sigma_k^2 - n\delta_{\max}^2\right)\rho}{1 + n\delta_{\max}^2(K-1)^2\rho}\right) \tag{7}$$

where $\delta_{\max}^2 \triangleq \max_{k,l} \delta_{kl}^2$, $\sigma_k^2 \triangleq \left\|\mathbf{U}_k^{\mathrm{H}}\hat{\mathbf{H}}_{kk}\mathbf{V}_k\right\|_2^2$ and $\rho \triangleq \frac{\varepsilon}{N_0}$ denote the maximum error bound, the desired signal power and signal to noise ratio (SNR) of transmitted symbol, respectively.

From (7), it is a challenge to estimate the value of $\delta_{\max}^2$, that is, δ_{kl}^2. In practical applications, LS or minimum mean square error (MMSE) CE algorithms are usually used in wireless communications [19]. Then, in the following two subsections, we focus on the LS and RMMSE CE algorithm and derive the detailed expression of lower bound of rate, the objective function in (6), with LS and RMMSE CE, respectively.

3.2 Derivation of Lower Bound of Rate with LS CE

In this subsection, we adopt LS CE algorithm with the optimal training signal [20]. In this case, the CE error under optimal training is given by [20]

$$\mathbb{E}\left\{\left\|\Delta\mathbf{H}_{kl}^{\mathrm{LS}}\right\|_{\mathrm{F}}^2\right\} = \mathbb{E}\left\{\left\|\mathbf{H}_{kl} - \hat{\mathbf{H}}_{kl}^{\mathrm{LS}}\right\|_{\mathrm{F}}^2\right\} = \frac{N_0 m^2 n}{\alpha T \varepsilon_{\mathrm{t}}} \tag{8}$$

where $\Delta\mathbf{H}_{kl}^{\mathrm{LS}}$ and $\mathbf{H}_{kl}^{\mathrm{LS}}$ represent the CE error matrix and estimated channel matrix based on LS CE algorithm, and ε_{t} denotes the transmitted power for training symbol. Note that there is no error in feeding back the CSI to all users.

From the definition of δ_{kl}^2 in (5), we easily have

$$\delta_{kl}^2 \le \left\|\mathbf{H}_{kl} - \hat{\mathbf{H}}_{kl}^{\mathrm{LS}}\right\|_{\mathrm{F}}^2. \tag{9}$$

Further, combining (3) and (8), and with the definition of $\delta_{\max}^2$ in (10), we have [21]

$$\begin{aligned} \delta_{\max}^2 &= \max_{k,l} \delta_{kl}^2 \\ &\le \frac{m^2 n N_0}{\alpha T \varepsilon_{\mathrm{t}}} = \frac{m^2 n}{\alpha T \rho_{\mathrm{t}}} \end{aligned} \tag{10}$$

where $\rho_{\mathrm{t}} \triangleq \frac{\varepsilon_{\mathrm{t}}}{N_0}$ denotes the SNR for training symbol.

Substituting (10) into (7) and with some simple calculations, we can formulate the lower bound of achievable rate for the k-th user pair as

$$R_k^{\mathrm{L}}(\alpha) = (1-\alpha)\log_2\left(\frac{A\alpha + B}{C\alpha + D}\right) \tag{11}$$

where

$$\begin{aligned} A &= T\rho_{\mathrm{t}}\left(1 + \rho\sigma_k^2\right), \\ B &= m^2 n^2 \rho\left[(K-1)^2 - 1\right], \\ C &= T\rho_{\mathrm{t}}, \\ D &= m^2 n^2 \rho (K-1)^2. \end{aligned} \tag{12}$$

From (11), it can be observed that the lower bound of achievable rate, $R_k^{\mathrm{L}}(\alpha)$, is related but not monotonic to the TSF α.

3.3 Derivation of Lower Bound of Rate with RMMSE CE

In this subsection, we focus on the RMMSE CE algorithm which represents a simplified and approximated version of MMSE method. Different from traditional MMSE algorithm, RMMSE algorithm requires only the knowledge of the trace of the correlation matrix and the received noise power. We adopt RMMSE CE algorithm with the optimal training signal and the CE error is given by [20]

$$\begin{aligned} \mathbb{E}\left\{\left\|\Delta\mathbf{H}_{kl}^{\mathrm{RMMSE}}\right\|_{\mathrm{F}}^2\right\} &= \mathbb{E}\left\{\left\|\mathbf{H}_{kl} - \hat{\mathbf{H}}_{kl}^{\mathrm{RMMSE}}\right\|_{\mathrm{F}}^2\right\} \\ &= \frac{\mathrm{tr}\left(\mathbf{R}_{\mathbf{H}_{kl}}\right) m^2 n N_0}{\mathrm{tr}\left(\mathbf{R}_{\mathbf{H}_{kl}}\right) T\varepsilon_{\mathrm{t}}\alpha + m^2 n N_0} \end{aligned} \tag{13}$$

where $\Delta\mathbf{H}_{kl}^{\mathrm{RMMSE}}$ and $\mathbf{H}_{kl}^{\mathrm{RMMSE}}$ represent the CE error matrix and estimated channel matrix based on RMMSE CE algorithm, and $\mathbf{R}_{\mathbf{H}_{kl}} = \mathbb{E}\left\{\mathbf{H}_{kl}^{\mathrm{H}}\mathbf{H}_{kl}\right\}$ is the channel correlations matrix.

Similar to (9) in Sec. 3.2, we have

$$\delta_{kl}^2 \le \left\|\mathbf{H}_{kl} - \hat{\mathbf{H}}_{kl}^{\mathrm{RMMSE}}\right\|_{\mathrm{F}}^2 \tag{14}$$

and

$$\begin{aligned} \delta_{\max}^2 &= \max_{k,l} \delta_{kl}^2 \\ &\le \frac{\mathrm{tr}\left(\mathbf{R}_{\mathbf{H}_{kl}}\right) m^2 n N_0}{\mathrm{tr}\left(\mathbf{R}_{\mathbf{H}_{kl}}\right) T\varepsilon_{\mathrm{t}}\alpha + m^2 n N_0} \\ &= \frac{\mathrm{tr}\left(\mathbf{R}_{\mathbf{H}_{kl}}\right) m^2 n}{\mathrm{tr}\left(\mathbf{R}_{\mathbf{H}_{kl}}\right) T\rho_{\mathrm{t}}\alpha + m^2 n}. \end{aligned} \tag{15}$$

Substituting (15) into (7) and with some simple calculations, we can get the lower bound of achievable rate for the k-th user pair $R_k^{\mathrm{L}}(\alpha)$ with RMMSE CE which has the same form as (11). However, the values of A, B, C and D are

different from (12) and can be computed as

$$\begin{aligned} A &= T\rho_{\mathrm{t}}\mathrm{tr}\left(\mathbf{R}_{\mathbf{H}_{kl}}\right)\left(1+\rho\sigma_k^2\right), \\ B &= m^2 n\left(1+\rho\sigma_k^2\right)+m^2n^2\rho\mathrm{tr}\left(\mathbf{R}_{\mathbf{H}_{kl}}\right)\left[(K-1)^2-1\right], \\ C &= T\rho_{\mathrm{t}}\mathrm{tr}\left(\mathbf{R}_{\mathbf{H}_{kl}}\right), \\ D &= m^2 n+m^2n^2\rho\mathrm{tr}\left(\mathbf{R}_{\mathbf{H}_{kl}}\right)(K-1)^2. \end{aligned} \tag{16}$$

3.4 Existence of Optimal TSF

From (11), (12) and (16), it can be seen that the optimal solution for (6) is difficult to calculate. Before solving the optimization problem, we must first validate the existence of optimum. Consequently, we calculate the second order derivative of $R_k^{\mathrm{L}}(\alpha)$ with respect to α as

$$\frac{\mathrm{d}^2R_k^{\mathrm{L}}(\alpha)}{\mathrm{d}^2\alpha}=\frac{1+\ln 2}{\ln 2}E+\frac{1-\alpha}{\ln 2}F \tag{17}$$

where

$$\begin{aligned} E &= \frac{C}{C\alpha+D}-\frac{A}{A\alpha+B}=\frac{BC-AD}{(A\alpha+B)(C\alpha+D)}, \\ F &= \frac{C^2}{(C\alpha+D)^2}-\frac{A^2}{(A\alpha+B)^2} \\ &= \frac{\left(B^2C^2-A^2D^2\right)+2AC(BC-AD)\alpha}{(A\alpha+B)^2(C\alpha+D)^2}. \end{aligned} \tag{18}$$

From (11), we can easily prove that $0<B<D$ and $0<C<A$ for both LS and RMMSE CE algorithm. Therefore, we have

$$\begin{aligned} &BC-AD<0, \\ &B^2C^2-A^2D^2<0, \\ &(A\alpha+B)(C\alpha+D)>0. \end{aligned} \tag{19}$$

With (19), we further have $E<0$ and $F<0$. Then, considering $\alpha\in(0,1)$, we can prove $\frac{\mathrm{d}^2R_k^{\mathrm{L}}(\alpha)}{\mathrm{d}^2\alpha}<0$, which indicates a maximum for $R_k^{\mathrm{L}}(\alpha)$ exists. Here, in order to find the maximum and the optimal TSF, we can take the first order derivative of $R_k^{\mathrm{L}}(\alpha)$ with respect to α and set it to zero; and then we can obtain the following equation about α as

$$\begin{aligned} \frac{\mathrm{d}R_k^{\mathrm{L}}(\alpha)}{\mathrm{d}\alpha} &= \frac{1-\alpha}{\ln 2}\left(\frac{A}{A\alpha+B}-\frac{C}{C\alpha+D}\right) \\ &\quad+\log_2\left(\frac{C\alpha+D}{A\alpha+B}\right)=0. \end{aligned} \tag{20}$$

From (20), we have

$$\frac{\mathrm{d}R_k^{\mathrm{L}}(\alpha)}{\mathrm{d}\alpha}\Big|_{\alpha=1}=\log_2\left(\frac{C+D}{A+B}\right)=\log_2\left(1+\frac{G}{A+B}\right) \tag{21}$$

and

$$\frac{\mathrm{d}R_k^{\mathrm{L}}(\alpha)}{\mathrm{d}\alpha}\Big|_{\alpha=0}=\frac{1}{\ln 2}\left(\frac{AD-BC}{BD}\right)+\log_2\left(\frac{D}{B}\right) \tag{22}$$

where

$$G=\begin{cases} -T\rho_{\mathrm{t}}\rho\sigma_k^2+m^2n^2\rho, & \text{LS CE} \\ -\left[T\rho_{\mathrm{t}}\rho\mathrm{tr}\left(\mathbf{R}_{\mathbf{H}_{kl}}\right)+m^2n\rho\right]\sigma_k^2 \\ \quad+m^2n^2\rho\mathrm{tr}\left(\mathbf{R}_{\mathbf{H}_{kl}}\right), & \text{RMMSE CE.} \end{cases} \tag{23}$$

When the SNR for training symbol ρ_{t} is large enough, we can prove $G<0$ for both LS and RMMSE CE algorithms; then we can further prove $\frac{\mathrm{d}R_k^{\mathrm{L}}(\alpha)}{\mathrm{d}\alpha}\big|_{\alpha=1}<0$.

As for (22), because $0<B<D$ and $0<C<A$ for both LS and RMMSE CE algorithm, we have $AD-BC>0$. Consequently, we can obtain $\frac{\mathrm{d}R_k^{\mathrm{L}}(\alpha)}{\mathrm{d}\alpha}\big|_{\alpha=0}>0$.

From (20), $\frac{\mathrm{d}R_k^{\mathrm{L}}(\alpha)}{\mathrm{d}\alpha}$ is a continuous function about α. Therefore, from the analysis above, the optimal TSF $\alpha_{\mathrm{opt}}\in(0,1)$ satisfying (20) exists.

3.5 Solution for the Optimization Problem

The existence of optimal TSF is proven in previous subsection. And we can find α_{opt} by solving (20). However, from (20), the equation includes a complicated logarithmic operation, which makes the equation more difficult to be solved. Moreover, due to the involvement of α^2 in (20), W-Lambert function [22], [23] cannot be applied to get the solution. The theoretical optimal TSF, α_{opt}, can be determined by the root of (20), which can be solved easily using Matlab but difficultly for practical application. Actually, we can utilize the traversal searching method to obtain the optimal TSF in $(0,1)$ with a small step. Besides, we also want to propose another simplified algorithm to solve the equation in (20). In our previous work, we used Taylor expansion to reduce the complexity of the solution [24], [25]. Here, we also introduce Taylor expansion to approximate the Logarithm function in (20) which effectively reduces the computational complexity and only brings some small and acceptable errors validated in the following simulations. The Taylor expansion can be express as

$$\begin{aligned} \ln(k) &= \ln\left(\frac{1+\frac{k-1}{k+1}}{1-\frac{k-1}{k+1}}\right)=2\arctan\left(\frac{k-1}{k+1}\right) \\ &= 2\sum_{n=1}^{\infty}\frac{1}{2n-1}\left(\frac{k-1}{k+1}\right)^{2n-1} \end{aligned} \tag{24}$$

where $k=\frac{C\alpha+D}{A\alpha+B}$, $\left|\frac{k-1}{k+1}\right|<1$ for all values of α and ρ .

Obviously, the term $\frac{1}{2n-1}\left(\frac{k-1}{k+1}\right)^{2n-1}$ in (24) is rapidly decreasing with the increase of n. Thus, in the following analysis, $\ln(k)$ can be approximated with only the first term

in (24) with small and acceptable error. Then, the logarithmic item in (20) is approximately represented as

$$\log_2\left(\frac{C\alpha+D}{A\alpha+B}\right) \approx \frac{2}{\ln 2} \times \frac{\frac{C\alpha+D}{A\alpha+B}-1}{\frac{C\alpha+D}{A\alpha+B}+1}. \tag{25}$$

Substituting (25) into (20), we can obtain the detailed approximated representation for (20) as

$$a_1\alpha^3 + a_2\alpha^2 + a_3\alpha + a_4 = 0 \tag{26}$$

where

$$\begin{aligned} a_1 &= 2AC(C-A), \\ a_2 &= 3(AD+BC)(C-A), \\ a_3 &= 5BD(C-A) + AD(A+C+D) - BC(A+B+C), \\ a_4 &= 2BD(D-B) - (B+D)(BC-AD). \end{aligned} \tag{27}$$

In the following part, we will present some simulation results to verify the acceptance of small approximation errors compared to the theoretical computing results.

4. Numerical Results and Analysis

In this section, we present some numerical results to verify the correctness of the proposed optimization scheme. In the simulation, we set $m = 2$, $n = 2$, $K = 3$, $T = 100T_s$ (here T_s denotes the symbol period), and $\sigma_k^2 = 1$. Define the ratio of the transmitted SNRs for training and data symbols as $\mu = \rho/\rho_t$. And for simplification, assume that $\mu = 1$ for equal power allocation for the training and data symbols except for Fig. 8 and Fig. 9. All elements in $\mathbf{H}_{kl}$ are further assumed to be complex Gaussian distributed random variables with zeros mean and unit variance for $k, l = 1, 2, \cdots, K$. All the derivations and simulations can be directly extended to other configurations of m, n, and K.

Figure 2 and Figure 3 show the lower bound of achievable rate $R_k^{\mathrm{L}}(\alpha)$ versus TSF α for different transmitted symbol SNR ρ with LS and RMMSE CE, respectively. From Fig. 2 and Fig. 3, it can be observed that, for the same TSF α, the lower bound of achievable rate, $R_k^{\mathrm{L}}(\alpha)$, increases with the increase of ρ. This is consistent with the results we expected. However, from (11), when $\alpha = 0$, $R_k^{\mathrm{L}}(\alpha)\big|_{\alpha=0} = \log_2\left(\frac{B}{D}\right)$ has no relationship with ρ; and when $\alpha = 1$, $R_k^{\mathrm{L}}(\alpha) = 0$. Both $R_k^{\mathrm{L}}(\alpha)\big|_{\alpha=1}$ and $R_k^{\mathrm{L}}(\alpha)\big|_{\alpha=0}$ are constants. For a certain ρ, the lower bound of achievable rate, $R_k^{\mathrm{L}}(\alpha)$, first increases then decreases as α increases. When α is small, as the α increases, the estimated channel matrix $\hat{\mathbf{H}}_{kl}$ becomes more precise and the interference leakage due to the CE error decreases. Thus, the lower bound of achievable rate first increases. However, when α increases up to a certain value, the increase of α can improve the precision of CE slightly but brings out the decrease of the lower bound of achievable rate due to shorter data transmission duration $(1-\alpha)T$. Consequently, $R_k^{\mathrm{L}}(\alpha)$ decreases as α increases.

From Fig. 2 and Fig. 3, we also discover that, there is a maximum of the lower bound of rate and a corresponding optimal TSF for a given ρ. Moreover, with the increase of ρ, the channel becomes better, and shorter duration can generate precise enough CE. This means higher value of ρ results in smaller value of α_{opt}.

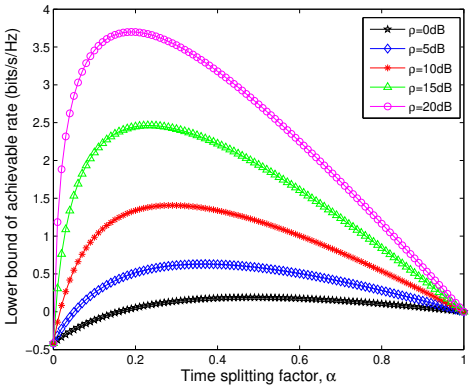

Fig. 2. Lower bound of achievable rate $R_k^{\mathrm{L}}(\alpha)$ with LS CE versus TSF α for different transmitted symbol SNR ρ.

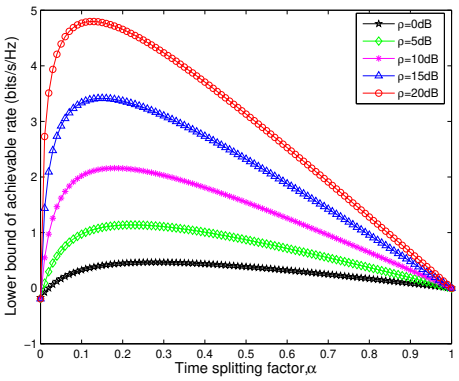

Fig. 3. Lower bound of achievable rate $R_k^{\mathrm{L}}(\alpha)$ with RMMSE CE versus TSF α for different transmitted symbol SNR ρ.

ρ in dB	Theoretical	Simulated	Approximated
0	0.4842	0.484	0.485
5	0.3656	0.366	0.367
10	0.2891	0.289	0.299
15	0.2325	0.233	0.246
20	0.1906	0.191	0.213

Tab. 1. Comparison of theoretical, simulated and approximated time splitting factors with LS CE, α_{opt}s, for different values of ρ.

ρ in dB	Theoretical	Simulated	Approximated
0	0.2763	0.276	0.277
5	0.2230	0.223	0.231
10	0.1816	0.182	0.205
15	0.1497	0.150	0.193
20	0.1261	0.126	0.189

Tab. 2. Comparison of theoretical, simulated and approximated time splitting factors with RMMSE CE, α_{opt}s, for different values of ρ.

In Tab. 1 and Tab. 2, we compare the theoretical TSF directly calculated from (20), the simulated TSF from Fig. 3 and the approximated TSF calculated from (26) for different values of ρ with LS and RMMSE CE algorithms, respectively. From Tab. 1 and Tab. 2, we conclude that the theoretical and simulated α_{opt}s are almost same for all values of ρ, where the small difference attributes to the simulation step for α; whereas the simulated and approximated α_{opt}s have some small differences resulting from the limited items of Taylor expansion in (25).

Figure 4 shows the simulated optimal TSF α_{opt} versus transmitted symbol SNR ρ. It can be seen that α_{opt} decreases as ρ increases for both LS and RMMSE CE algorithm. As expected, the lower the SNR is, the longer training duration is required to provide a better estimation. As the SNR increases, shorter training duration is needed. In addition, we also discover that, the simulated optimal TSF α_{opt} with RMMSE CE is smaller than α_{opt} with LS CE, which indicates RMMSE CE algorithm needs shorter training duration than LS CE algorithm does for the same SNR in order to maximize the lower bound of achievable rate. This also contribute to the superiority of RMMSE CE over LS CE in terms of achievable rate.

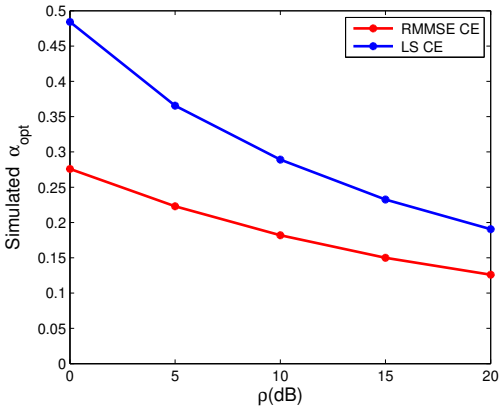

Fig. 4. Simulated optimal TSF α_{opt} versus transmitted symbol SNR ρ.

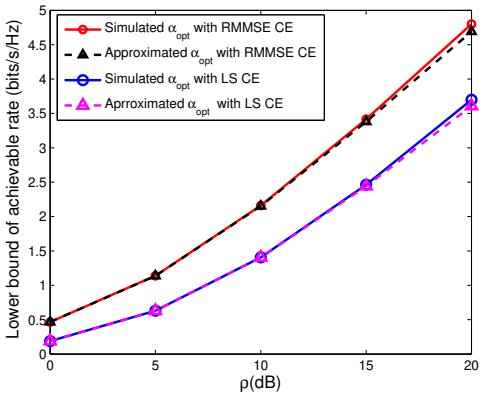

Fig. 5. Optimized lower bound of achievable rate $R_k^{\text{L}}(\alpha_{\text{opt}})$ versus transmitted symbol SNR ρ.

Figure 5 shows the optimized lower bound of achievable rate, $R_k^{\text{L}}(\alpha_{\text{opt}})$, versus the transmitted symbol SNR ρ. For comparison, we plot the simulated and approximated lower bound of achievable rates by substituting the simulated α_{opt} and the approximated α_{opt} into (11), respectively. We can discover that the simulated and approximated rates coincide well with each other and with some acceptable and small gaps. Therefore, considering the difficulty to calculate the theoretical α_{opt} from (20), the approximated α_{opt} from (26) can be used to maximize the lower bound of achievable rate in practical applications.

From Fig. 5, it also can be seen that the optimized lower bound of achievable rate $R_k^{\text{L}}(\alpha_{\text{opt}})$ with RMMSE CE is higher than that with LS CE for all SNRs which indicates RMMSE CE algorithm is better that LS CE algorithm in the IA based network.

Figure 6 and Figure 7 illustrate the lower bounds of achievable rate under the optimal TSF α_{opt} and some fixed TSFs with LS and RMMSE CE, respectively. We can discover that the optimal TSF α_{opt} can achieve larger rate over other fixed TSFs due to its adaptivity to the channel characteristics and its statistics of CE errors. In addition, RMMSE CE algorithm shows better performance than LS CE because RMMSE considers noise statistics as modification.

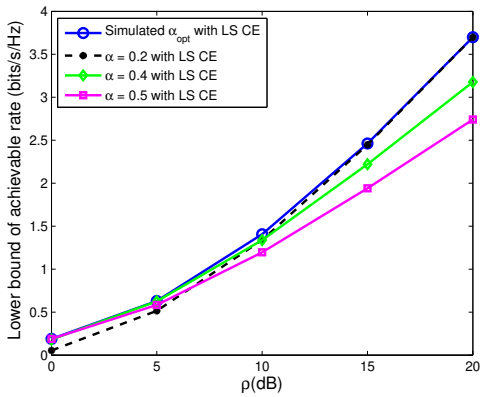

Fig. 6. Comparison of the lower bounds of achievable rate under different TSFs with LS CE.

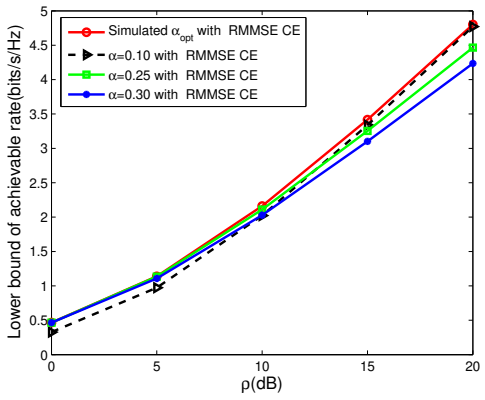

Fig. 7. Comparison of the lower bounds of achievable rate under different TSFs with RMMSE CE.

In the previous simulation, we consider the symmetrical case, where the training and data symbols' transmissions have the same power ($\mu = 1$), i.e., $\rho_t = \rho$. In the following two figures, we evaluate the optimal TSF α_{opt} and lower bound of achievable rate for asymmetrical case, that is, $\mu \neq 1$.

Figure 8 shows the simulated optimal TSF α_{opt} with RMMSE CE versus transmitted symbol SNR ρ under different values of μ. From Fig. 8, we can discover that, for a certain ρ, smaller μ means higher training symbol SNR ρ_t; as a result, shorter training duration is required to provide a better enough CE.

Figure 9 shows the optimized lower bound of achievable rate $R_k^L(\alpha_{opt})$ with RMMSE CE versus the transmitted symbol SNR ρ under different values of μ. As expected, we can discover that the smaller μ is, the higher optimized lower bound of achievable rate is for all values of ρ. This improvement attributes to better CE with higher training symbol SNR ρ_t for smaller μ.

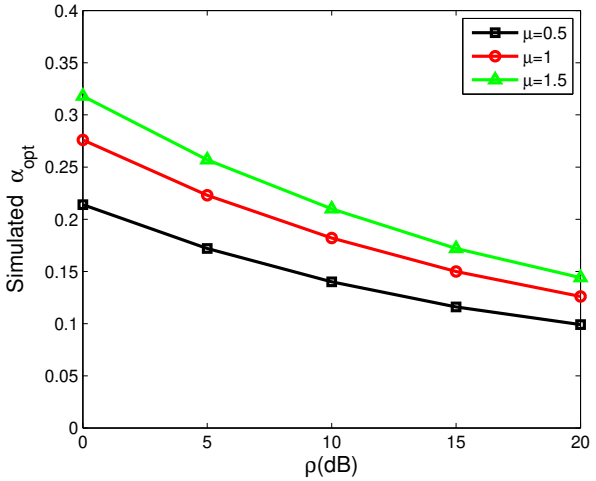

Fig. 8. Simulated optimal TSF α_{opt} with RMMSE CE versus transmitted symbol SNR ρ under different values of μ.

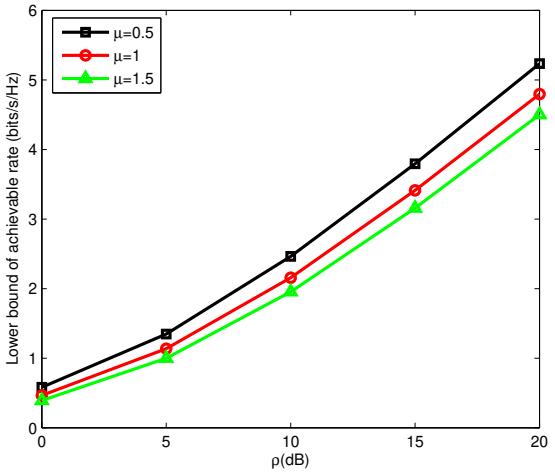

Fig. 9. Optimized lower bound of achievable rate $R_k^L(\alpha_{opt})$ with RMMSE CE versus transmitted symbol SNR ρ under different values of μ.

5. Conclusions

In this paper, we have studied an optimized time splitting scheme to improve the system performance in an IA based network with consideration of the practical CE algorithms. In order to lower down the optimization complexity, we introduce the lower bound of achievable rate as an optimization indicator and the Taylor expansion for approximation. With the numerical results and their correpsonding analysis, we discover that the optimized TSF can improve the system rate compared with the traditional fixed TSFs due to its adaptivity to the channel characteristics and its statistics of CE errors. In addition, the RMMSE CE algorithm shows better performance than the LS CE algorithm because the RMMSE CE considers noise statistics as modification. Furthermore, the approximation of optimal TSF just brings out some small and acceptable errors on the system rate. In our future work, we plan to consider to perform the optimization jointly combining power allocation and time splitting between the training and data symbols.

Acknowledgments

This work was supported in part by the National Natural Science Foundation of China (No. 61501376, 61701407, and 61871327), the Science and Technology Program of Shenzhen, China (No. JCYJ20170306155652174), the Natural Science Basic Research Plan in Shaanxi Province of China (No. 2018JM6037 and 2018JQ6017), the Fundamental Research Funds for the Central Universities (No. 3102018JGC006 and 3102017JG02002), the Aeronautical Science Foundation of China (2017ZC53029) and the Graduate Starting Seed Fund of Northwestern Polytechnical University (No. ZZ2018128).

References

[1] JAFAR, S. A., SHAMAI, S. Degrees of freedom region for the MIMO X channel. *IEEE Transactions on Information Theory*, 2007, vol. 54, no. 1, p. 151–170. ISSN: 0018-9448. DOI: 10.1109/TIT.2007.911262

[2] CADAMBE, V. R., JAFAR, S. A. Interference alignment and degrees of freedom of the K-user interference channel. *IEEE Transactions on Information Theory*, 2008, vol. 54, no. 8, p. 3425–3441. ISSN: 0018-9448. DOI: 10.1109/TIT.2008.926344

[3] YAO, R., LIU, Y., LU, L., et al. Cooperative precoding for cognitive transmission in two-tier networks. *IEEE Transactions on Communications*, 2016, vol. 64, no. 4, p. 1423–1436. ISSN: 0090-6778. DOI: 10.1109/TCOMM.2016.2536027

[4] GOMADAM, K., CADAMBE, V. R., JAFAR, S. A. A distributed numerical approach to interference alignment and applications to wireless interference networks. *IEEE Transactions on Information Theory*, 2011, vol. 57, no. 6, p. 3309–3322. ISSN: 0018-9448. DOI: 10.1109/TIT.2011.2142270

[5] NOSRAT-MAKOUEI, B., ANDREWS, J. G., HEATH, R. W. MIMO interference alignment over correlated channels with imperfect CSI. *IEEE Transactions on Signal Processing*, 2011, vol. 59, no. 6, p. 2783–2794. ISSN: 1053-587X. DOI: 10.1109/TSP.2011.2124458

[6] LI, X., ZHAO, N., SUN, Y., et al. Interference alignment based on antenna selection with imperfect channel state information in cognitive radio networks. *IEEE Transactions on Vehicular Technology*, 2016, vol. 65, no. 7, p. 5497–5511. ISSN: 0018-9545. DOI: 10.1109/TVT.2015.2439300

[7] AQUILINA, P., RATNARAJAH, T. Linear interference alignment in full-duplex MIMO networks with imperfect CSI. *IEEE Transactions on Communications*, 2017, vol. 65, no. 12, p. 5226–5243. ISSN: 0090-6778. DOI: 10.1109/TCOMM.2017.2744647

[8] AYACH, O. E., LOZANO, A., HEATH, R. W. On the overhead of interference alignment: Training, feedback, and cooperation. *IEEE Transactions on Wireless Communications*, 2012, vol. 11, no. 11, p. 4192–4203. ISSN: 1536-1276. DOI: 10.1109/TWC.2012.092412120588

[9] GUIAZON, R. F., WONG, K. K., WISELY, D. Capacity analysis of interference alignment with bounded CSI uncertainty. *IEEE Wireless Communications Letters*, 2014, vol. 3, no. 5, p. 505–508. ISSN: 2162-2337. DOI: 10.1109/LWC.2014.2344656

[10] GUIAZON, R. F., WONG, K. K., FITCH, M. Capacity distribution for interference alignment with CSI errors and its applications. *IEEE Transactions on Wireless Communications*, 2016, vol. 15, no. 1, p. 1–10. ISSN: 1536-1276. DOI: 10.1109/TWC.2015.2477298

[11] KHAN, M. N., GILANI, S. O., JAMIL, M., et al. Maximizing Throughput of Hybrid FSO-RF Communication System: An Algorithm. *IEEE Access*, 2018, vol. 6, p. 30039–30048. ISSN: 2169-3536. DOI: 10.1109/ACCESS.2018.2840535

[12] HASSAN, H., KHAN, M. N., GILANI, S. O., et al. H.264 Encoder Parameter Optimization for Encoded Wireless Multimedia Transmissions. *IEEE Access*, 2018, vol. 6, p. 22046–22053. ISSN: 2169-3536. DOI: 10.1109/ACCESS.2018.2824835

[13] MALIK, M. H., JAMIL, M., KHAN, M. N., et al. Formal modelling of TCP congestion control mechanisms ECN/RED and SAP-LAW in the presence of UDP traffic. *EURASIP Journal on Wireless Communications and Networking*, 2016, vol. 2016, no. 1, p.22046–22053. ISSN: 1687-1499. DOI: 10.1186/s13638-016-0646-9

[14] YAO, R., LU, Y., TSIFTSIS, T. A., et al. Secrecy rate-optimum energy splitting for an untrusted and energy harvesting relay network. *IEEE Access*, 2018, vol. 6, p. 19238–19246. ISSN: 2169-3536. DOI: 10.1109/ACCESS.2018.2819639

[15] WU, Y., WANG, T., SUN, Y., et al. Time allocation optimisation for multi-antenna wireless information and power transfer with training and feedback. *IET Communications*, 2017, vol. 11, no. 3, p. 414–420. ISSN: 1751-8628. DOI: 10.1049/iet-com.2016.0425

[16] YAO, R., GAO, Y., XU, J., et al. Impact of channel estimation error on upper bound of rate loss for macro cell in a VFDM system. In *Proceedings of the 26th Wireless and Optical Communications Conference (WOCC)*. Newark (USA), 2017, p. 1–5. ISSN: 2379-1276. DOI: 10.1109/WOCC.2017.7928999

[17] ZHENG, G., WONG, K. K., OTTERSTEN, B. Robust cognitive beamforming with bounded channel uncertainties. *IEEE Transactions on Signal Processing*, 2009, vol. 57, no. 12, p. 4871–4881. ISSN: 1053-587X. DOI: 10.1109/TSP.2009.2027462

[18] MEKKAWY, T., YAO, R., XU, F., et al. Optimal power allocation in an amplify-and-forward untrusted relay network with imperfect channel state information. *Wireless Personal Communications*, 2018, vol. 101, no. 3, p. 1281–1293. ISSN: 09296212. DOI: 10.1007/s11277-018-5762-x

[19] SAHU, A., KHARE, A. A Comparative analysis of LS and MMSE channel estimation, techniques for MIMO-OFDM system. *International Journal of Engineering Research and Applications*, 2014, vol. 4, no. 6, p. 162–167. ISSN: 2248-9622

[20] BIGUESH, M., GERSHMAN, A. B. Training-based MIMO channel estimation: a study of estimator tradeoffs and optimal training signals. *IEEE Transactions on Signal Processing*, 2006, vol. 54, no. 3, p. 884–893. ISSN: 1053-587X. DOI: 10.1109/TSP.2005.863008

[21] GUIAZON, R. F., WONG, K. K., FITCH M. Evolution of capacity lower bound of interference alignment with least-square channel estimation. In *Proceedings of the 3th IEEE China Summit and International Conference on Signal and Information Processing (ChinaSIP)*. Chengdu (China), 2015, p. 582–585. DOI: 10.1109/ChinaSIP.2015.7230470

[22] SBOUI, L., REZKI, Z., ALOUINI, M. S. Energy-efficient power allocation for MIMO-SVD systems. *IEEE Access*, 2017, vol. 5, p. 9774–9784. ISSN: 2169-3536. DOI: 10.1109/ACCESS.2017.2707550

[23] LEI, W. J., JIANG, X., ZUO, L. J., et al. A secure transmission scheme for wireless energy harvesting aystems via energy cooperation and cooperative jamming. *Acta Electronica Sinica*, 2017, vol. 45, no. 1, p. 67–73. DOI: 10.3969/j.issn.0372-2112.2017.01.010

[24] YAO, R., LI, T., LIU, Y., et al. Analytical approximation of the channel rate for massive MIMO system with large but finite number of antennas. *IEEE Access*, 2018, vol. 6, no. 99, p. 6496–6504. ISSN: 2169-3536. DOI: 10.1109/ACCESS.2017.2787668

[25] YAO, R., MEKKAWY, T., XU, F. Optimal power allocation to increase secure energy efficiency in a two-way relay network. In *Proceedings of the 2017 IEEE 86th Vehicular Technology Conference (VTC-Fall)*. Toronto (Canada), 2017, p. 1–5. DOI: 10.1109/VTCFall.2017.8288198

About the Authors . . .

Rugui YAO (corresponding author) received his B.Sc., M.Sc., and Ph.D. degrees in Telecommunications and Information Systems from the School of Electronics and Information (SEI), Northwestern Polytechnical University (NPU), Xi'an, China, in 2002, 2005, and 2007, respectively. From 2007 to 2009, he worked as a post-doctoral fellow at NPU. Since 2009, he has been with SEI, NPU, Xian, China, where he is now an associate professor. In 2013, he joined ITP Lab at Georgia Tech, Atlanta, USA, as a visiting scholar. He has worked in the areas of cognitive radio networks, channel coding, OFDM transmission, and physical layer security. He is a member of the IEEE and a senior member of the Chinese Institute of Electronics.

Lukun YAO received her B.Sc. degree in Communication Engineering from the School of Electronics and Information (SEI), Northwestern Polytechnical University (NPU), Xi'an, China, in 2017. From 2017 to 2018, she studies as a postgraduate in Telecommunications and Information Systems from the School of Electronics and Information, Northwestern Polytechnical University, Xi'an, China. Her research interests include wireless communications and interference alignment.

Juan XU received the B.Sc., M.Sc., and Ph.D degrees all in the School of Computer from Northwestern Polytechnical University (NPU), China, in 2002, 2005 and 2011, respectively. From 2011, she joined the School of Electronic and Control Engineering at Chang'an University, Xi'an, China and became an associate professor in 2015. Her research interests include channel coding, OFDM transmission and spread spectrum systems.

Xiaoya ZUO received the B.Sc., M.Sc., and Ph.D. degrees in Communication Engineering from Northwestern Polytechnical University, Xi'an, China, in 2005, 2008, and 2011, respectively. He is currently an associate professor at the School of Electronics and Information (SEI), Northwestern Polytechnical University (NPU). From 2008 to 2009, he was a Visiting Scholar at the Department of Electrical and Computer Engineering, University of Victoria, Victoria, BC, Canada. His research interests include broadband wireless communications, ultra-wideband communications, millimeter wave communication systems, and multiple-input multiple-output communication systems.

Hailong LIU received the B.Sc., M.Sc., and Ph.D. degrees all in the School of Computer Science from Northwestern Polytechnical University (NPU), China, in 2002, 2005 and 2011, respectively. Now he is an associate professor in NPU. He is the member of ACM SIGMOD China and Database Technical Committee of China Computer Federation. His research interests include signal processing, big data management and data quality.